

# Mutation of a chloroplast-targeting signal in *Alternanthera* mosaic virus TGB3 impairs cell-to-cell movement and eliminates long-distance virus movement

Hyoun-Sub Lim,<sup>1†</sup> Anna Maria Vaira,<sup>1,2†</sup> Hanhong Bae,<sup>3</sup>  
Jennifer N. Bragg,<sup>4</sup> Steven E. Ruzin,<sup>5</sup> Gary R. Bauchan,<sup>6</sup>  
Margaret M. Dienelt,<sup>1</sup> Robert A. Owens<sup>1</sup> and John Hammond<sup>1</sup>

## Correspondence

John Hammond  
John.Hammond@ars.usda.gov

<sup>1</sup>USDA-ARS, Plant Sciences Institute, Molecular Plant Pathology Laboratory, B-004, 10300 Baltimore Avenue, Beltsville, MD 20705, USA

<sup>2</sup>CNR, Istituto di Virologia Vegetale, Strada delle Cacce 73, Torino 10135, Italy

<sup>3</sup>School of Biotechnology, Yeungnam University, Geongsan 712-749, Republic of Korea

<sup>4</sup>USDA-ARS, Western Regional Research Center, 800 Buchanan Street, Albany, CA 94710, USA

<sup>5</sup>University of California-Berkeley, CNR, 381 Koshland Hall, Berkeley, CA 94720, USA

<sup>6</sup>USDA-ARS, Plant Sciences Institute, Electron and Confocal Microscopy Unit, B-465, 10300 Baltimore Avenue, Beltsville, MD 20705, USA

Cell-to-cell movement of potexviruses requires coordinated action of the coat protein and triple gene block (TGB) proteins. The structural properties of *Alternanthera* mosaic virus (AltMV) TGB3 were examined by methods differentiating between signal peptides and transmembrane domains, and its subcellular localization was studied by *Agrobacterium*-mediated transient expression and confocal microscopy. Unlike potato virus X (PVX) TGB3, AltMV TGB3 was not associated with the endoplasmic reticulum, and accumulated preferentially in mesophyll cells. Deletion and site-specific mutagenesis revealed an internal signal VL(17,18) of TGB3 essential for chloroplast localization, and either deletion of the TGB3 start codon or alteration of the chloroplast-localization signal limited cell-to-cell movement to the epidermis, yielding a virus that was unable to move into the mesophyll layer. Overexpression of AltMV TGB3 from either AltMV or PVX infectious clones resulted in veinal necrosis and vesiculation at the chloroplast membrane, a cytopathology not observed in wild-type infections. The distinctive mesophyll and chloroplast localization of AltMV TGB3 highlights the critical role played by mesophyll targeting in virus long-distance movement within plants.

Received 21 December 2009

Accepted 10 April 2010

## INTRODUCTION

Plant viruses rely on the availability of connections between cells and the vascular system and utilize the resources of the endogenous host trafficking systems, such as cytoskeleton, endoplasmic reticulum (ER) and Golgi, to facilitate movement in a susceptible host and establish a successful infection. Viral genomes encode proteins that have evolved to achieve these functions (Leisner & Howell, 1993; Lucas, 2006; Verchot-Lubicz *et al.*, 2007). Research on the mechanisms of plant virus movement has provided insight into the interactions that must occur with the host for the

virus to move into adjacent cells (Boevink & Oparka, 2005; Lucas, 2006; Waigmann *et al.*, 2004). In addition to viral movement proteins, some viral RNAs also have a role in systemic invasion (Ding *et al.*, 1996; Lough *et al.*, 2006).

For mechanically transmitted viruses, such as potexviruses, infection initiated in epidermal cells spreads by cell-to-cell movement via mesophyll and bundle sheath cells to the phloem parenchyma and companion cells. Steps involved in virus entry and exit from the sieve elements (Ding, 1998; Haywood *et al.*, 2002; Lough & Lucas, 2006; Lucas *et al.*, 2001) are still poorly understood; however, isolation of mutants that can move from cell to cell but not systemically suggests that phloem-dependent transport involves interactions separate from those involved in cell-to-cell movement (Dolja *et al.*, 1994; Xiong *et al.*, 1993).

†These authors contributed equally to this work.

Two supplementary tables and two supplementary figures are available with the online version of this paper.

Several groups of viruses encode a 'triple gene block' (TGB) of movement-related proteins. These have been differentiated into 'class I' hordei-like viruses, which have rigid, rod-shaped particles, and 'class II' potex-like viruses, having flexuous particles [exemplified by *Potato virus X* (PVX), type member of the genus *Potexvirus*] (reviewed by Morozov & Solovyev, 2003). Potexviruses have positive-sense, single-stranded, monopartite RNA genomes of approximately 5.9–7.0 kb with five gene products (Adams *et al.*, 2004; Fig. 1a); other well-studied members include *White clover mosaic virus* (WClMV), *Papaya mosaic virus* (PapMV), *Foxtail mosaic virus* (FMV) and *Bamboo mosaic virus* (BaMV). *Alternanthera mosaic virus* (AltMV) is related most closely to PapMV (Geering & Thomas, 1999; Hammond *et al.*, 2006).

Several reports have addressed the contributions of TGB proteins to movement for WClMV (Lough *et al.*, 1998), PVX (Ju *et al.*, 2005; Krishnamurthy *et al.*, 2003; Lough *et al.*, 2000; Solovyev *et al.*, 2000; Tamai & Meshi, 2001) and BaMV (Lin *et al.*, 2006), and describe *trans* complementation of potexviral genomes with defects within the TGB through delivery of functional TGB constructs by using particle bombardment (Morozov *et al.*, 1997), transgenic plants (Lough *et al.*, 1998) or satellite RNA (Lin *et al.*, 2006). Despite this body of work, 'a full understanding of the specific requirement of TGB3 and the functional interchangeability of TGB3 among different potexviruses for intercellular movement remains elusive' (Lin *et al.*, 2006).

The 8 kDa PVX TGB3 is an ER-binding protein with a single, N-terminal transmembrane domain (Morozov & Solovyev, 2003; Verchot-Lubicz *et al.*, 2007), and TGB2 and TGB3 are reported to co-localize (Ju *et al.*, 2008; Solovyev *et al.*, 2000). PVX TGB3 interacts with the ER network and is associated with granular vesicles induced by TGB2 (Samuels *et al.*, 2007). The 7 kDa TGB3 of AltMV is similar in size to that of PVX (Hammond *et al.*, 2006), but appears to behave differently.

Here, we compare subcellular-localization patterns of AltMV and PVX TGB3 fusion proteins expressed in *Nicotiana benthamiana* leaves by agroinfiltration and show that AltMV TGB3 has properties distinct from those reported for other potexvirus TGB3 proteins. AltMV TGB3 preferentially accumulates near the chloroplast membrane in mesophyll cells and appears to facilitate virus movement between different cell types.

## RESULTS

### Subcellular localization of PVX and AltMV TGB3

Subcellular localization of several class I (hordeivirus-like) and class II (potexvirus-like) TGB proteins has been investigated by using fluorescent gene fusions (Haupt *et al.*, 2005; Ju *et al.*, 2005; Lim *et al.*, 2009; Lough *et al.*, 1998; Solovyev *et al.*, 2000). To assess localization of AltMV TGB3, we

expressed TGB3 from pGDR and pGDG (Goodin *et al.*, 2002) or pHVLR and pHVLG vectors for *Agrobacterium*-mediated transient expression of DsRed or green fluorescent protein (GFP) fusions (Fig. 1b). Agroinfiltrated *N. benthamiana* leaves were evaluated for fluorescent protein expression by laser-scanning confocal microscopy (LSCM) and differential interference contrast (DIC) at 2–3 days post-infiltration. Western blots (Fig. 1c) confirmed stable expression of the fusion proteins. Epidermal and mesophyll cells were visualized separately in the same leaf using LSCM by focusing on images at different depths within the Z-stack, and in the transverse sections (Fig. 1e–k).

Transient expression of AltMV DsRed–TGB3 and PVX DsRed–TGB3 are shown (in red) in Fig. 1(e–j). Transverse sections and optical sections at different depths from the adaxial surface were observed. Epidermal cells were recognized by their location at the leaf surface, irregular shape and essential absence of chloroplasts. Elongated-globular palisade mesophyll cells containing numerous chloroplasts (green fluorescence in Fig. 1e–j; red fluorescence in Fig. 1k) were observed beneath the adaxial epidermis. DsRed–TGB3<sub>PVX</sub> localized at epidermal and mesophyll cell membranes, surrounding nuclei and in the cytoplasmic network of both layers, conforming to reported associations with ER and cell membranes (Ju *et al.*, 2008) (Fig. 1e–g). In contrast, DsRed–TGB3<sub>AltMV</sub> localized almost exclusively to the mesophyll layer, as punctate fluorescent foci (Fig. 1h–j). DsRed–TGB3<sub>AltMV</sub> was rarely detected in the epidermal layer (0–20 µm) in either transverse or Z-stack sections, but was detected readily within mesophyll cells; in optical sections, most DsRed–TGB3<sub>AltMV</sub> fluorescence was detected at about 40 µm depth. GFP–TGB3<sub>AltMV</sub> showed a similar distribution (data not shown).

When pGDR–TGB3 (DsRed–TGB3<sub>AltMV</sub>) and pGDG–TGB3<sub>PVX</sub> (GFP–TGB3<sub>PVX</sub>) were co-agroinfiltrated, the calculated lateral image from a Z-stack image of 40 optical slices of 1 µm from the adaxial epidermis into the mesophyll layer clearly differentiated localization of DsRed–TGB3<sub>AltMV</sub> (shown as green) and GFP–TGB3<sub>PVX</sub> (shown as grey). TGB3<sub>AltMV</sub> was concentrated in the mesophyll layer at 20–40 µm, whereas TGB3<sub>PVX</sub> was observed at between 0 and 20 µm in epidermal cells (Fig. 1k).

Because localization of PVX GFP–TGB2 and GFP–TGB3 is altered by co-expression of PVX TGB3 (Schepetilnikov *et al.*, 2005; Solovyev *et al.*, 2000), we co-expressed free AltMV TGB2, TGB2 + TGB3 or TGB3 (from pGD–TGB2, pGD–TGB2/3 and pGD–TGB3, respectively; Fig. 1d) with DsRed–TGB3<sub>AltMV</sub>. No alteration of DsRed–TGB3 localization was observed (data not shown).

### Comparative analysis of AltMV and other potexvirus TGB3 sequences

BLASTP analysis of the AltMV TGB3 amino acid sequence showed limited similarity to potexvirus homologues, with

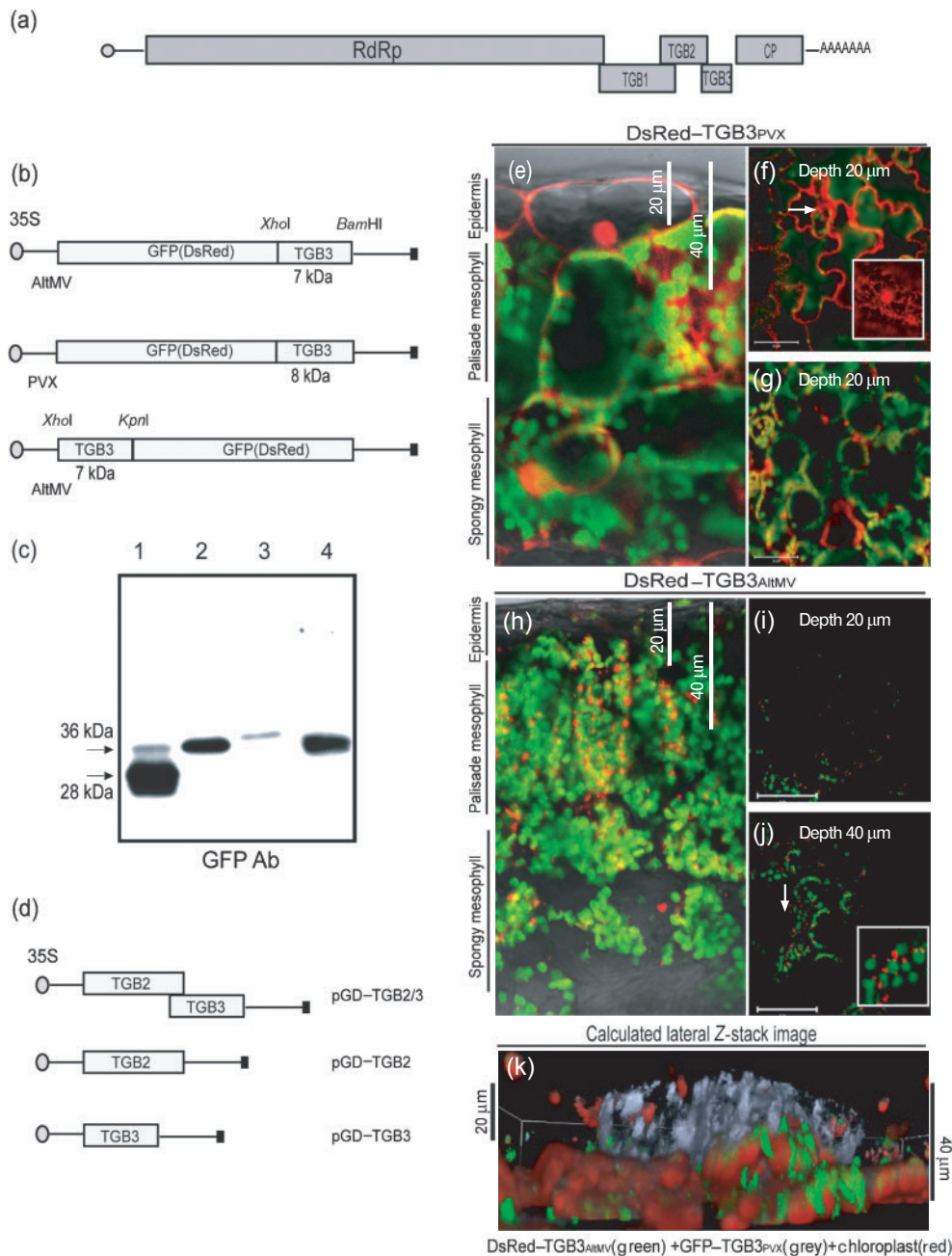


**Fig. 1.** Transient expression of TGB3 fusion proteins in *N. benthamiana*. (a) Genome organization of AltMV. (b) pGDG (GFP-TGB3), pGDR (DsRed-TGB3), pHLV (TGB3-GFP) and pHLR (TGB3-DsRed) TGB3<sub>AltMV</sub> and TGB3<sub>PVX</sub> fusion constructs. (c) Western blot with anti-GFP antibodies (Ab) of agroinfiltrated leaf extracts separated by SDS-PAGE (12% gel). Lanes: 1, pGDG (GFP); 2, pGDG-TGB3<sub>AltMV</sub>; 3, pGDG-TGB3<sub>PVX</sub>; 4, pHLR-TGB3<sub>AltMV</sub>. Arrows indicate positions of standards. (d) pGD constructs for agroinfiltration of TGB2/3, TGB2 and TGB3. (e-k) *N. benthamiana* tissue agroinfiltrated with pGDR-TGB3<sub>PVX</sub> (e-g), pGDR-TGB3<sub>AltMV</sub> (h-j) or pGDR-TGB3<sub>AltMV</sub> plus pGDG-TGB3<sub>PVX</sub> (k). Transverse sections (e, h) and optical sections at 20  $\mu$ m (f, i) and 40  $\mu$ m (g, j) depth (0  $\mu$ m, top of epidermis). Chloroplast autofluorescence is shown as green (e-j). (e-g) DsRed-TGB3<sub>PVX</sub> was observed in both epidermal and mesophyll cells, at the cell periphery and ER network; the inset in (f) shows a magnified image of the arrowed area. (h-j) DsRed-TGB3<sub>AltMV</sub> was localized to mesophyll cells; the magnified inset in (j) shows the association with chloroplasts. (k) pGDR-TGB3<sub>AltMV</sub> and pGDG-TGB3<sub>PVX</sub> were co-infiltrated; a calculated projection of 40 optical slices (Z-stack) from the adaxial epidermis illustrates separation of GFP-TGB3<sub>PVX</sub> (grey) in the epidermal layer from DsRed-TGB3<sub>AltMV</sub> (green) and chloroplast autofluorescence (red) primarily in the mesophyll layer. Bars (f, g, i, j), 50  $\mu$ m.

only 42% identity to PapMV TGB3 and 38% identity to just the C-terminal region of tulip virus X (TVX) TGB3. Additional gaps were introduced into a CLUSTAL alignment of the TGB3 amino acid sequences of AltMV, PVX and other potexviruses to optimize alignment of the TGB3 'signature motif' (Morozov *et al.*, 1991). TGB3 proteins of TVX and *Plantago asiatica* mosaic virus (PIAMV) have significantly extended N termini, and that of PIAMV an extended C terminus, whilst FMV and BaMV TGB3 proteins have shorter C termini relative to AltMV TGB3 (Fig. 2). The TGB3 'signature motif', C(X<sub>5</sub>)G(X<sub>6-9</sub>)C (Morozov *et al.*, 1991; Morozov & Solovyev, 2003), was present in all sequences.

The pfam02495 7 kDa viral coat protein (CP) domain identified in many potex- and carlavirus TGB3 sequences was variously complete [clover yellow mosaic virus (CIYMV), WCIMV], truncated (PVX, TVX, PIAMV) or not recognized (AltMV and other viruses; see Supplementary Table S2, available in JGV Online).

The Phobius software package has been shown to improve differentiation of signal peptides (SPs) from transmembrane domains (Käll *et al.*, 2004, 2005). AltMV, PapMV, CIYMV, FMV and zygocactus virus X (ZVX) TGB3 proteins were predicted by Phobius to have N-terminal SPs, whilst PVX, WCIMV, TVX and PIAMV TGB3 proteins were predicted to have N-terminal transmembrane domains; the BaMV TGB3 N-terminal domain prediction was inconclusive (Fig. 2; Supplementary Table S2). Predicted transmembrane domains of TVX and PIAMV TGB3 proteins were internal to the N terminus, corresponding to the aligned transmembrane domains of PVX and WCIMV TGB3 proteins (Fig. 2).

PVX TGB3 has predicted 23 aa N-terminal transmembrane and C-terminal 45 aa cytoplasmic segments (Krishnamurthy *et al.*, 2003). SignalP identified both the PVX TGB3 N-terminal 23 aa and the AltMV TGB3 N-terminal 20 aa as SPs. TargetP identified both PVX and AltMV TGB3s as

secretory pathway-directed, whereas ChloroP did not identify either as chloroplast-transit peptides.

The differences in predicted structure and observed localization of AltMV and PVX TGB3 proteins led us to examine the features of AltMV TGB3 responsible.

### AltMV TGB3 accumulates in the mesophyll and contains a novel signal for chloroplast membrane localization

To analyse further the importance of AltMV TGB3 amino acid sequences in mesophyll localization, C-terminal fusions of AltMV TGB3 were created (Fig. 3a) in binary vectors pHVLG and pHVLR (TGB3-GFP; TGB3-DsRed) in addition to N-terminal fusions GFP-TGB3 and DsRed-TGB3. Localization of transiently expressed fusion proteins (Fig. 3a) was evaluated. Expression of wild-type (WT) TGB3 as an N- or C-terminal fusion did not change its localization in the mesophyll compared with the epidermis, but affected localization at the chloroplast level (Fig. 3b, c); GFP-TGB3 or DsRed-TGB3 localized as punctate foci associated closely with chloroplasts (Fig. 3b), whilst TGB3-DsRed or TGB3-GFP formed partial or complete fluorescent haloes around the chloroplasts (Fig. 3c). These localizations are distinct from native GFP or DsRed accumulation in mesophyll cells (not shown), presumably reflecting the position of TGB3 exposure in the fusion protein.

A series of deletion mutants (N- or C-terminal fusions; Fig. 3a) was produced in order to identify residues required for chloroplast or mesophyll targeting. Residues 17–18 (i.e. VL), overlapping the C-terminal portion of the predicted AltMV TGB3 SP, were required (but not necessarily sufficient) for chloroplast targeting. Mutant TGB3ΔN20, lacking this sequence, accumulated in epidermal cells, whereas TGB3ΔN9 and TGB3ΔN16ΔC11 did not and were retained at the chloroplast (Fig. 3a, d–f). TGB3ΔN9 also formed cytoplasmic granules (Fig. 3d) of unknown significance. Isolated chloroplasts were obtained for

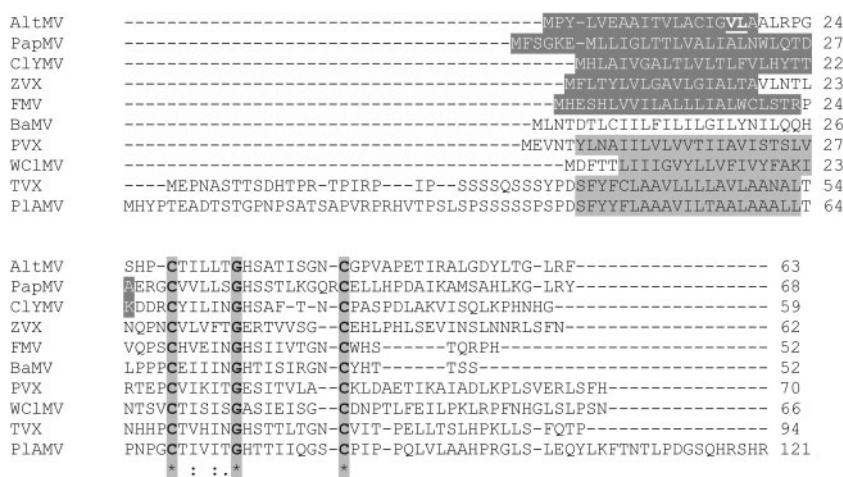


**Fig. 2.** CLUSTAL alignment of TGB3 of AltMV and other potexviruses. Additional gaps were introduced to maximize alignment of the TGB3 'signature motif' (shaded, bold letters; Morozov *et al.*, 1991; Morozov & Solovyev, 2003). Predicted SPs of AltMV, PapMV, CIYMV, ZVX and FMV (white lettering) and transmembrane domains of TVX, PIAMV, WCIMV and PVX are shaded, with AltMV residues VL(17,18) underlined.

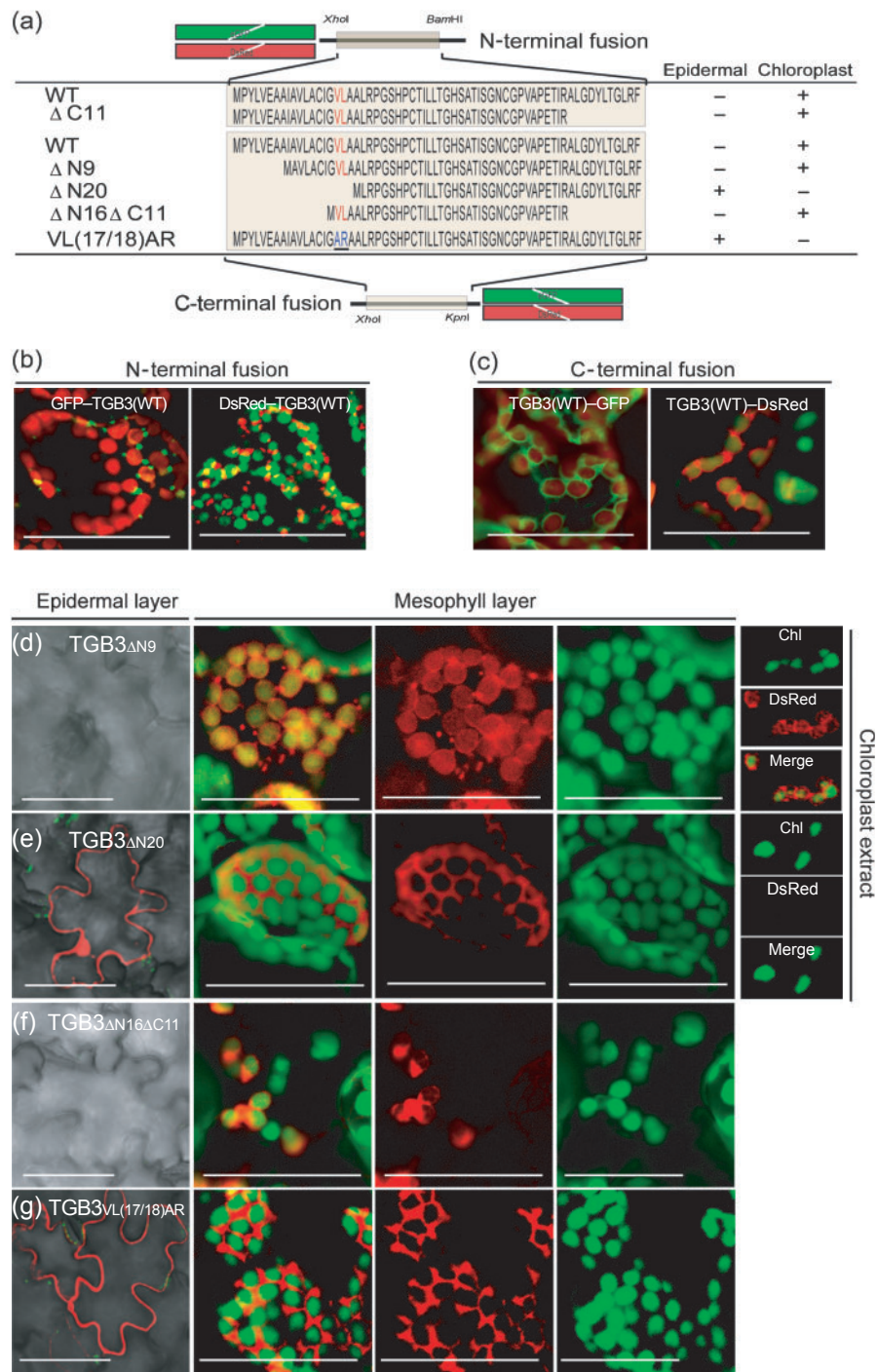


**Fig. 3.** Subcellular localization of AltMV TGB3 mutants. (a) N- and C-terminal TGB3 deletion mutants were introduced into pGDG, pGDR, pHVLR and pHVLR; amino acid sequences maintained in the fusion proteins are shown. (b–g) Constructs were transiently expressed in *N. benthamiana* by agroinfiltration and examined by LSCM at 36 h post-infiltration to detect fluorescent protein expression and chloroplast autofluorescence (shown in red with GFP fusions and in green with DsRed fusions). (b) WT GFP-TGB3 and DsRed-TGB3; (c) WT TGB3-GFP and TGB3-DsRed. (d–g) Expression of mutants from pHVLR (TGB3-DsRed). Epidermal layer: combined DsRed and DIC image. Mesophyll layer: left, combined DsRed and chloroplast autofluorescence; centre, DsRed; right, chloroplast autofluorescence. Far right: chloroplasts extracted from leaf tissue by chopping in water (upper: autofluorescence; middle: DsRed; lower: merge); (d) TGB3 $\Delta$ N9; (e) TGB3 $\Delta$ N20; (f) TGB3 $\Delta$ N16 $\Delta$ C11; (g) TGB3<sub>VL(17/18)AR</sub>. Bars, 50  $\mu$ m.

LSCM by cutting tissue in water, and chloroplast association of VL-containing TGB3–DsRed variants (WT,  $\Delta N9$ ,  $\Delta N16\Delta C11$ ) was readily detected. In contrast, deletion  $\Delta N20$  (lacking VL) was not associated with isolated chloroplasts (Fig. 3d, e, far right panels).

Mutation of residues 17–18 was sufficient to ablate formation of chloroplast-associated foci; TGB3<sub>VL(17,18)AR</sub>–DsRed showed epidermal and mesophyll expression similar to that of free DsRed, without chloroplast localization (compare Fig. 3g with Fig. 3c, d).

### AltMV TGB2, TGB3, CP and the TGB3 VL(17,18) signal involved in chloroplast targeting are each required for systemic movement

In order to evaluate the contributions of TGB2, TGB3, the apparent TGB3 chloroplast-localization signal and CP in cell-to-cell movement, infectious clone AltMV–enhanced (e)GFP (Fig. 4a) was modified to knock out expression of the TGB2, TGB3 or CP open reading frames (ORFs) by mutation of their respective initiation codons or the TGB3 chloroplast signal [TGB3<sub>VL(17,18)AR</sub>]. Mutant transcripts were inoculated onto the adaxial leaf surface of *N. benthamiana*. WT AltMV–eGFP was detected at both adaxial and abaxial epidermal surfaces at 5 days post-inoculation (p.i.), and in the mesophyll; horizontal movement reached 1000  $\mu\text{m}$  diameter within 7 days p.i., followed by systemic infection (Fig. 4b). TGB2- and CP-defective viruses (AltMV $\Delta$ TGB2–eGFP, AltMV $\Delta$ CP–eGFP) infected only single epidermal cells without further movement, and diffusion of free GFP from infected cells was not detected (Fig. 4c, f), similar to studies with WCLMV and PVX (Beck *et al.*, 1991; Lough *et al.*, 2000). Surprisingly, limited epidermal cell-to-cell movement of AltMV $\Delta$ TGB3–eGFP and AltMV.TGB3(VL17/18AR)–eGFP was detected, with infection foci expanding to 700  $\mu\text{m}$  or less at 7 days p.i. (Fig. 4d, e).

Cell-to-cell movement was compared between WT and mutants by examination of eGFP distribution at 3 and 6 days p.i. AltMV $\Delta$ CP showed no movement beyond single cells (Fig. 4g), whereas AltMV.TGB3(VL17/18AR)–eGFP showed limited epidermal movement within 6 days p.i. (Fig. 4h). AltMV–eGFP showed multidirectional movement (Fig. 4i).

### Complementation of infectious clone AltMV $\Delta$ TGB3 *in trans* and *in cis*

GFP expression from AltMV $\Delta$ TGB3–eGFP in each cell was uniform (Fig. 4d) and distinct from the single-cell GFP expression observed with AltMV $\Delta$ TGB2 and AltMV $\Delta$ CP (Fig. 4c, f); however, no eGFP was detected beyond the epidermis. Examination of a Z-stack image beginning in the upper (adaxial) epidermis and extending into the mesophyll layer showed that eGFP expression in these foci was concentrated at the periphery of epidermal cells (Fig. 5a), with none observed in the underlying mesophyll or the abaxial surface (Fig. 5b, c). The calculated lateral image

showed clearly that AltMV $\Delta$ TGB3–eGFP was confined to the epidermal layer, with total separation from chloroplast autofluorescence in the mesophyll (Fig. 5d).

Impaired cell-to-cell movement of AltMV $\Delta$ TGB3–eGFP could be complemented *in trans* by free TGB3 via agroinfiltration of pGD–TGB3 4 days after inoculation with AltMV $\Delta$ TGB3–eGFP transcripts. At 7 days p.i., multidirectional movement had occurred, with AltMV $\Delta$ TGB3–eGFP detected in many mesophyll cells and both epidermal surfaces within agroinfiltrated regions (Fig. 5e–g). The calculated lateral image (Fig. 5h) demonstrated overlap of eGFP expression with mesophyll cell chloroplasts, confirming TGB3 complementation and movement within the agroinfiltrated leaf. No systemic movement was observed, as TGB3 agroinfiltration was localized.

As pGD–TGB3 was able to complement movement of AltMV $\Delta$ TGB3 within the agroinfiltrated leaf, we also expressed TGB3 *in cis* as an additional gene inserted into AltMV to examine complementation of both cell-to-cell and systemic movement. Two constructs were engineered: AltMV $\Delta$ TGB3(TGB3+) and AltMV $\Delta$ TGB3(TGB3–GFP+) (Fig. 5i, j). AltMV $\Delta$ TGB3(TGB3+) was able to infect plants systemically, inducing mild vein-associated symptoms (Fig. 5i), demonstrating that TGB3 expressed *in cis* was active for both cell-to-cell and systemic movement. In contrast, AltMV $\Delta$ TGB3(TGB3–GFP+) was able to spread locally within the inoculated leaf, infecting both upper and lower epidermis (Fig. 5j–l). No visible symptoms were apparent in non-inoculated leaves, and CP was barely detectable (Fig. 5j); thus TGB3–GFP was competent for local movement, but not for effective long-distance movement. TGB3–GFP localization from AltMV $\Delta$ TGB3(TGB3–GFP+) was not affected by the presence of native TGB2 (data not shown).

### Symptoms associated with overexpression of TGB3 are consistent with chloroplast damage

Infectious clone AltMV<sub>3-1</sub>, which produces mild symptoms (Lim *et al.*, 2010a), was modified to overexpress TGB3 as an added gene. AltMV<sub>3-1</sub>(TGB3<sub>AltMV</sub>+) induced significantly more severe symptoms than AltMV<sub>3-1</sub>, including veinal necrosis from 10 to 15 days p.i. Western blots demonstrated that levels of virus replication were comparable (Fig. 6a, b), whereas quantitative (Q)-RT-PCR results showed that AltMV(TGB3<sub>AltMV</sub>+) produced 6.5 ( $\pm 2.97$ ) times more TGB3 RNA than AltMV<sub>3-1</sub> (statistically significant at  $P=0.05$  by ANOVA; data not shown). PVX TGB3 was similarly overexpressed in AltMV<sub>3-1</sub>, but AltMV<sub>3-1</sub>(TGB3<sub>PVX</sub>+) did not induce severe symptoms (Fig. 6c, d). AltMV TGB3 or His-tag-modified TGB3 was also overexpressed from PVX-MCS (Fig. 6f, i). WT PVX induced mosaic in *N. benthamiana* and chlorotic local lesions in *Nicotiana tabacum* (Fig. 6e). At 10 days p.i., PVX(TGB3<sub>AltMV</sub>–His+) showed distinctive veinal necrosis in *N. benthamiana* and necrotic local lesions in *N. tabacum* (Fig. 6f) and, by 30 days p.i., the region of veinal necrosis had become bleached, with significantly

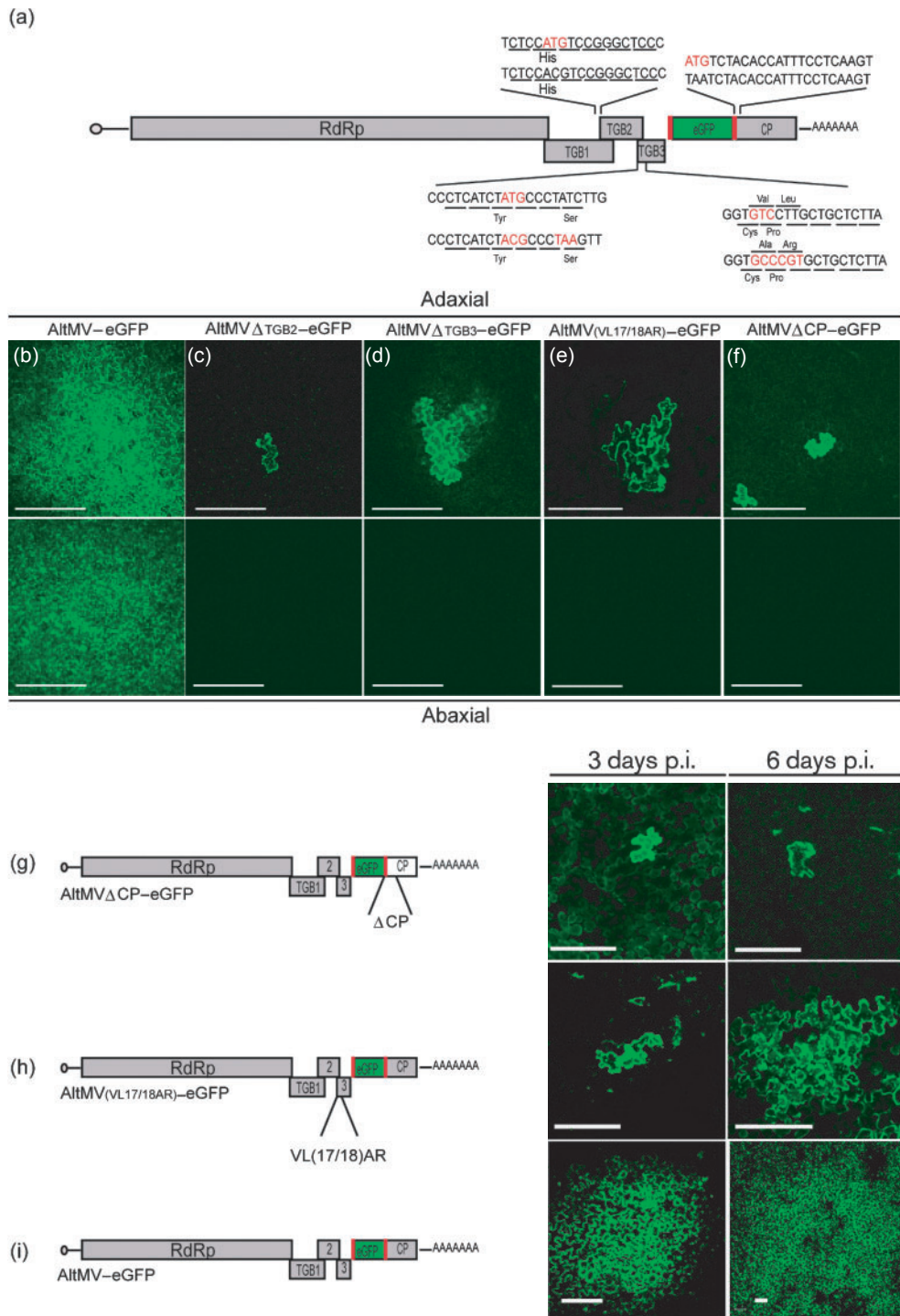


**Fig. 4.** Cell-to-cell spread of AltMV-eGFP and derivatives. (a) AltMV-eGFP was modified separately to prevent expression of TGB2, TGB3 or CP. For AltMVΔTGB2-eGFP, the TGB2 sequence was mutated without disrupting the TGB1 ORF (TGB1 codons underlined). For AltMVΔTGB3-eGFP and AltMV-TGB3<sub>VL(17/18)AR</sub>-eGFP, the TGB3 sequence was mutated without disrupting the TGB2 ORF (TGB2 codons underlined, TGB3 codons in red). (b-f) RNA transcripts were inoculated to *N. benthamiana* leaves (adaxial side) and LSCM images of adaxial (upper image) and abaxial (lower image) surfaces were captured at 7 days p.i. (b) AltMV-eGFP; (c) AltMVΔTGB2-eGFP; (d) AltMVΔTGB3-eGFP; (e) AltMV-TGB3<sub>VL(17/18)AR</sub>-eGFP; (f) AltMVΔCP-eGFP. (g-i) Constructs were inoculated to *N. benthamiana*; at 3 days p.i., a 1×1 cm leaf piece was examined by LSCM, maintained for 3 days in water and re-examined. (g) AltMVΔCP-eGFP; (h) AltMV-TGB3<sub>VL(17/18)AR</sub>-eGFP; (i) AltMV-eGFP. Bars, 200 μm.

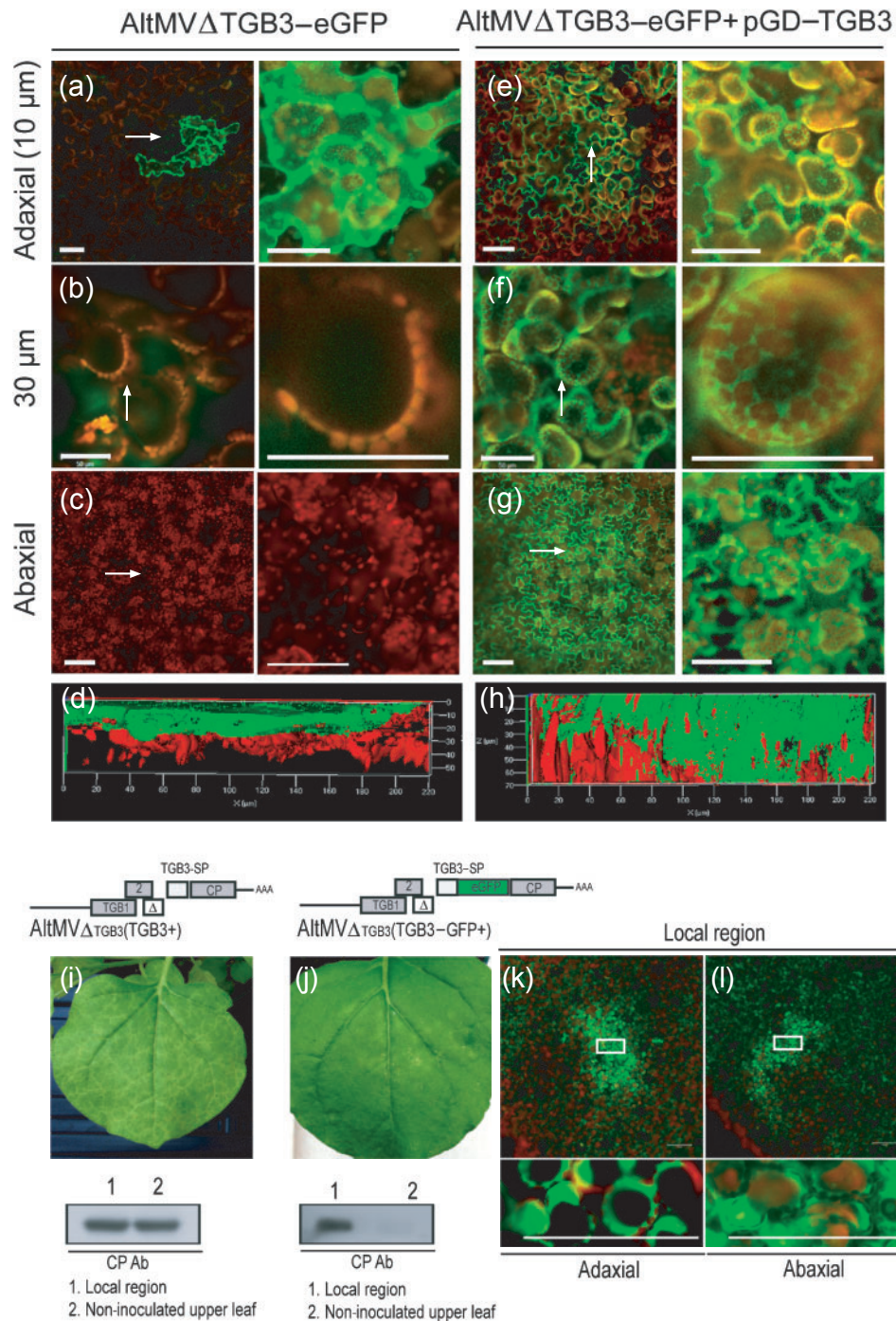


**Fig. 5.** *Trans* complementation of cell-to-cell spread of *AltMVΔTGB3-eGFP*. Transcripts were inoculated to *N. benthamiana* leaves (adaxial side), and LSCM images from adaxial (a, b, e, f) and abaxial (c, g) surfaces were captured at 7 days p.i. (a–d) *AltMVΔTGB3-eGFP*; (f–h) *AltMVΔTGB3-eGFP* followed 4 days p.i. by *pGD-TGB3* agroinfiltration. Right-hand panels are higher magnifications of the areas indicated by arrows. Bars, 50  $\mu$ m. (d, h) Calculated lateral images illustrate separation of signal from epidermal and mesophyll layers with *AltMVΔTGB3-eGFP* alone (d), but not when complemented by *pGD-TGB3* (h). (i) *AltMVΔTGB3(TGB3+)* transcript inoculation; overexpression of TGB3 as an added gene from *AltMV<sub>3-7</sub>ΔTGB3*. (j–l) *AltMVΔTGB3(TGB3-GFP+)*, overexpressing TGB-GFP from *AltMV<sub>3-7</sub>ΔTGB3* (j); transcripts were inoculated and inoculated tissue was examined by LSCM at 10 days p.i., from (k) adaxial and (l) abaxial sides (insets are magnified below). Bars, 200  $\mu$ m. (i, j) Western blots of inoculated and upper leaf samples (20 days p.i.) were developed with *AltMV* CP-specific antibody (Ab) after separation by SDS-PAGE (12% gel).

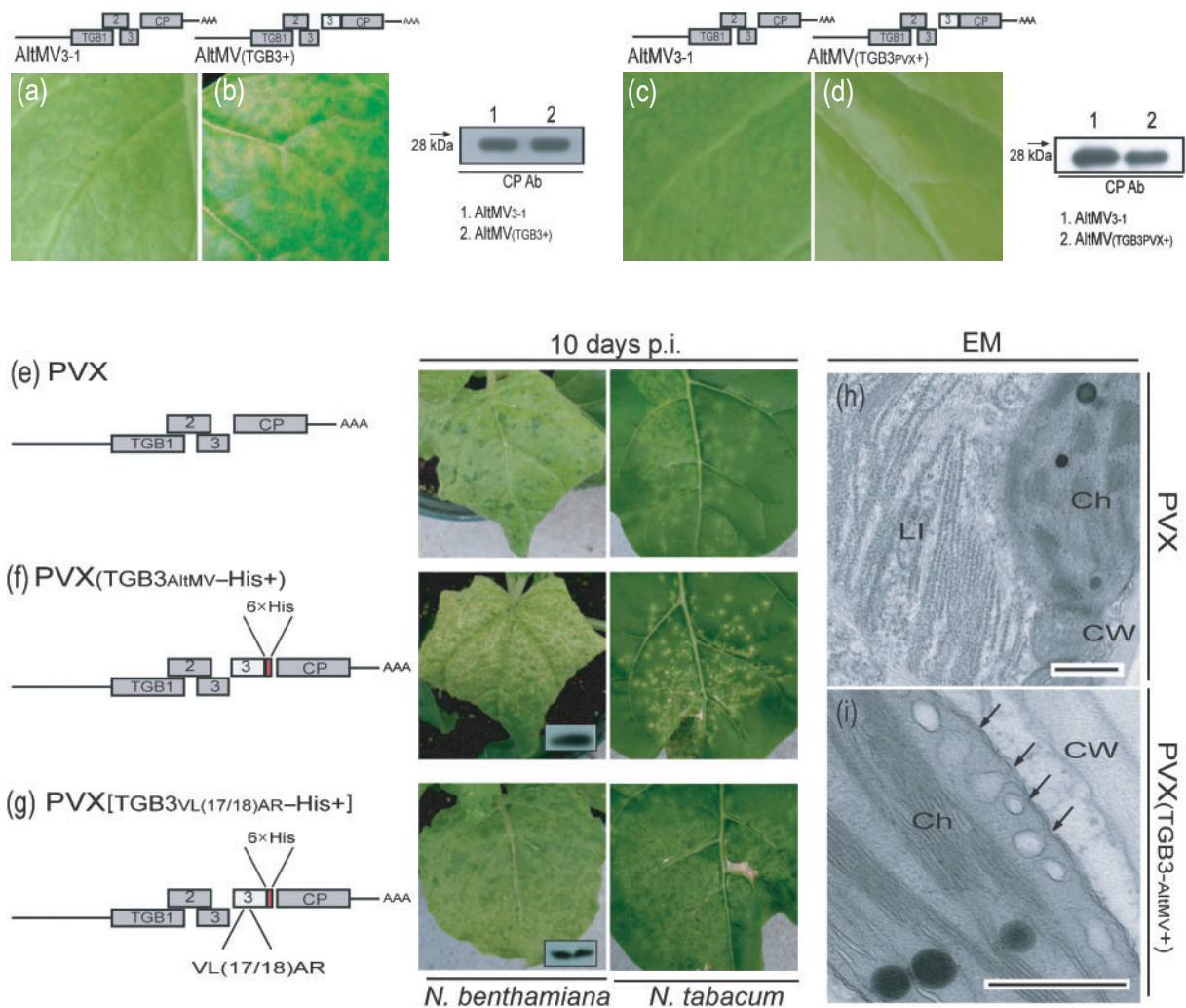


**Fig. 6.** TGB3 overexpressed from AltMV and PVX genomes as an additional gene. (a–d) Symptoms at 20 days p.i. of (a) WT mild AltMV<sub>3-1</sub>; (b) AltMV<sub>3-1</sub>(TGB3<sup>+</sup>) overexpressing AltMV TGB3 [veinal necrosis was observed in leaves and stems of *N. benthamiana* infected with AltMV<sub>3-1</sub>(TGB3<sup>+</sup>)]; (c) AltMV<sub>3-1</sub>; (d) AltMV(TGB3<sup>PVX+</sup>) overexpressing PVX TGB3. Protein extracts immunoblotted with AltMV CP-specific antibodies (Ab) following SDS-PAGE (12% gels) are also shown. (e–g) AltMV TGB3 overexpressed in PVX. (e) WT PVX; (f) PVX(TGB3<sup>AltMV</sup>-His<sup>+</sup>); (g) PVX[TGB3-His<sup>VL(17,18)AR</sup>+]. RNA transcripts were inoculated to *N. benthamiana* and *N. tabacum* and symptoms were recorded at 10 days p.i. (f, g) To confirm AltMV TGB3-His expression, extracts were immunoblotted with anti-His antibody following SDS-PAGE (20% gel) (inset). (h, i) Cytopathology was examined by electron microscopy. (h) WT PVX; (i) PVX(TGB3<sup>AltMV</sup>+); note unusual chloroplast vesiculations present only in plants overexpressing TGB3<sup>AltMV</sup>. CW, Cell wall; LI, laminated inclusions; Ch, chloroplast. Arrows indicate vesiculation of chloroplast membrane. Bars, 500 nm.

fewer chloroplasts (see Supplementary Fig. S1, available in JGV Online). Overexpression of TGB3<sup>VL(17,18)AR</sup>-His from PVX yielded symptoms similar to those of WT PVX in both *N. benthamiana* and *N. tabacum* (Fig. 6g). Electron microscopic observation of thin sections from young plant tissues infected with AltMV(TGB3<sup>AltMV</sup>+ ) and PVX(TGB3<sup>AltMV</sup>+ ) revealed major chloroplast malformations with vesicular invaginations of chloroplast membranes, and cytoplasmic membrane proliferation not present with WT PVX or AltMV<sub>3-1</sub> infections (Fig. 6i; Supplementary Fig. S2b, c).

Numbers of intact chloroplasts were compared by LSCM in symptomatic leaves infected by PVX and PVX(TGB3<sup>AltMV</sup>+ ). Significantly fewer chloroplasts were observed with PVX(TGB3<sup>AltMV</sup>+ ) than with WT PVX (Supplementary Fig. S1).

#### AltMV RNA also localizes around chloroplasts

Fluorescence *in situ* hybridization (FISH) was used to observe the distribution of AltMV RNA between the epidermis and mesophyll. Incubation of fluorescently

labelled AltMV-specific probe with transverse sections of AltMV-infected *N. benthamiana* leaf revealed widespread distribution of signal, with the highest intensity in the mesophyll; no signal was observed in non-inoculated control tissue (Fig. 7a, b). Closer examination revealed that signal in the epidermis was concentrated at the lower boundary of the cells, mainly in globular bodies consistent with chloroplasts; the signal in the mesophyll was also consistent with a distribution surrounding the chloroplasts (Fig. 7c–e), as for TGB3 (Fig. 3).

## DISCUSSION

Different potexviruses employ somewhat different mechanisms for cell-to-cell movement (Lin *et al.*, 2006). Previous studies have examined intracellular localization and interactions of the TGB proteins of several potexviruses through expression of individual gene fusion constructs by biolistic delivery to epidermal cells or expression from modified viral genomes (reviewed by Morozov & Solovyev, 2003; Verchot-Lubicz, 2005; Verchot-Lubicz *et al.*, 2007). In contrast, we have utilized *Agrobacterium*-mediated infiltration to deliver TGB fusion constructs throughout the leaf, and, in confirmatory experiments, expressed AltMV TGB3 variants as additional genes from both AltMV and PVX infectious clones. The behaviour of AltMV TGB3 in these assays clearly distinguishes it from those of PVX and WCIMV, the potexviruses for which the most detailed prior studies have been carried out.

Neither N- nor C-terminal fusions of AltMV TGB3 showed the ER-localization pattern observed with the PVX TGB3 control, which may assist TGB1 ribonucleoprotein complexes to plasmodesmata for cell-to-cell movement (Ju *et al.*, 2008; Verchot-Lubicz, 2005). AltMV TGB3–GFP expressed from AltMVΔTGB3(TGB3–GFP+) was able to complement local movement, and was therefore assumed to localize and function as does native TGB3 within the mesophyll, although lacking functionality for effective systemic movement through the vasculature. However, AltMV TGB3–(GFP or DsRed) and (GFP or DsRed)–TGB3 all localized to chloroplasts; localization was not affected by expression of free TGB2 or TGB3, unlike PVX GFP–TGB3 (Schepetilnikov *et al.*, 2005; Solovyev *et al.*, 2000). PVX GFP–TGB3 and DsRed–TGB3 mainly localized to the periphery of epidermal cells (this study), whereas PVX TGB3–GFP co-localized with replicase at spherical bodies along the ER (Bamunusinghe *et al.*, 2009) and not with chloroplasts.

To account for these differences, we compared predicted characteristics of TGB3 proteins of AltMV and other potexviruses, among which there is significant diversity (Lin *et al.*, 2006). Whereas SignalP identified an SP in both AltMV and PVX TGB3 proteins, Phobius analysis differentiated subclasses of TGB3 proteins, with AltMV-like TGB3 proteins having a predicted N-terminal SP, distinct from the PVX-like transmembrane domain. Many SPs are not cleaved, and uncleaved ‘signal anchors’ retain proteins in the targeted membrane (Sakaguchi *et al.*, 1992; von

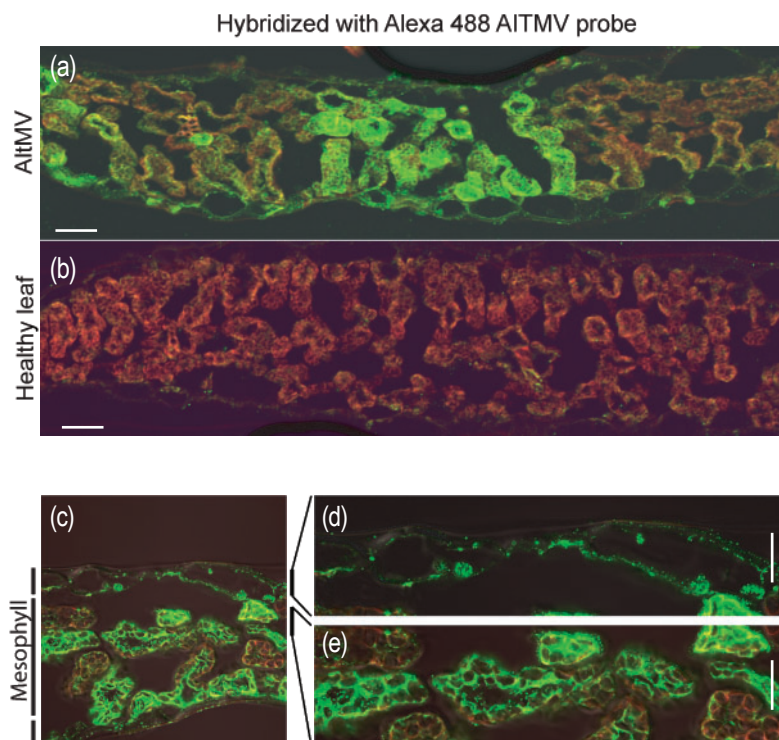


**Fig. 7.** Localization of viral RNA by FISH. *N. benthamiana* leaf tissue was processed for *in situ* hybridization using Alexa 488–UTP-labelled AltMV probe and examined by LSCM. (a) AltMV-infected tissue; (b) healthy leaf; (c) most of the signal was detected in mesophyll cells; (d) epidermal signal associated with chloroplasts; (e) stronger signal was detected around chloroplasts in mesophyll cells. Bars, 50  $\mu$ m (a–c); 20  $\mu$ m (d, e).

Heijne, 1988). The AltMV predicted SP is not cleaved, as agroinfiltrated TGB3–GFP(DsRed) and GFP(DsRed)–TGB3 were stable. Phobius may identify a signal anchor chloroplast-targeting signal, as AltMV (but not PVX) TGB3 fusions were directed to the chloroplast.

Deletion or mutation of TGB3 restricts replication of PVX (Lough *et al.*, 2000), WCIMV (Lough *et al.*, 1998) and BaMV (Lin *et al.*, 2006) to the inoculated cells, whereas systemic TGB3 complementation in transgenic plants enabled cell-to-cell and systemic movement (Lough *et al.*, 1998). In the case of AltMVΔTGB3–eGFP, infection spread beyond initially infected cells, but was restricted to the epidermis. Our data indicate that AltMV TGB3 is key for cell-to-cell movement and systemic infection through promoting virus entry to the mesophyll; complementation of AltMVΔTGB3–eGFP with agroinfiltrated TGB3 facilitated movement throughout the mesophyll and lower epidermis within the agroinfiltrated area. Deletion mutagenesis allowed us to identify VL(17,18) at the C-terminal end of the putative SP as crucial for both chloroplast binding and virus systemic movement.

Substitution VL(17,18)AR abolished the ability of TGB3–DsRed to bind to chloroplasts and ablated movement of AltMV<sub>VL(17,18)AR</sub>–eGFP from the epidermis to the mesophyll, suggesting a causal relationship between these processes. The importance of mesophyll targeting of AltMV was also demonstrated by FISH assay, showing that the chloroplast membrane is the preferential site for WT virus accumulation, making mesophyll invasion a critical step for virus infection.

Several reports describe virus interactions with chloroplasts, mainly relating to virus replication (Prod'homme *et al.*, 2003; Torrance *et al.*, 2006). Nevertheless, we show here for the first time that AltMV TGB3 is involved in transport between different cell types adjunct to replication. This distinction between AltMV and PVX may be compared with differences between distinct tombusviruses targeting either mitochondria or peroxisomes to form multivesicular bodies (Rubino & Russo, 1998), similar to the chloroplast vesiculation observed with AltMV TGB3 overexpression.

Overexpression of an individual viral protein can shed light on its function or target(s). Differences in the symptoms induced by overexpression of AltMV and PVX TGB3 from AltMV underline the difference between these two proteins; veinal necrosis was induced only where AltMV TGB3 was overexpressed. When overexpressed from a PVX vector, symptoms induced by TGB3<sub>VL(17,18)AR</sub>–His were very similar to those of WT PVX and only functional AltMV TGB3–His was able to induce necrosis in two distinct hosts. Electron microscopy of plants infected with PVX(TGB3<sub>AltMV</sub>+) revealed distinctive chloroplast membrane vesiculation not seen with WT PVX. Vascular association of TGB3 supports a role in systemic movement, whilst chloroplast vesiculation further supports the localization of fluorescent TGB fusions.

Native TGB3 is presumed to be produced from the same subgenomic (sg)RNA as TGB2, yielding coordinated production of these proteins. In the hordeivirus barley stripe mosaic virus (BSMV), TGB3 is produced in approximately one-tenth of the amount of TGB2 (Donald *et al.*, 1993). However, whilst excessive amounts of BSMV or other hordeivirus-like TGB3s interfere with virus replication (Lauber *et al.*, 2005; Lim *et al.*, 2008), there seems to be no such limitation with potexvirus-like TGB3s (Lin *et al.*, 2006; this study). The ability to overexpress TGB3 mutants *in cis* to complement a TGB3-defective AltMV should allow further examination of the functions of TGB3 for both local and long-distance movement, and of the differences between AltMV and PVX.

## METHODS

**Virus isolates and plant material.** AltMV isolate SP (AltMV-SP) was isolated from creeping phlox (*Phlox stolonifera* Sims) cv. Sherwood Purple (Hammond *et al.*, 2006) and maintained in *N. benthamiana* Domin by mechanical transfer. *N. benthamiana* plants were grown in 10 cm pots in a greenhouse at a nominal 22 °C/18 °C with supplementary lighting to extend the photoperiod to 14 h as necessary, or in growth chambers at 22 °C with a 16 h/8 h light/dark cycle. Three- to four-week-old *N. benthamiana* plants were used for virus infection and agroinfiltration.

**Construction of infectious AltMV cDNA clones.** All primers utilized in this work are shown in Supplementary Table S1, available in JGV Online. Construction of infectious clones AltMV<sub>3-1</sub> (mild), AltMV<sub>3-7</sub> (severe) and AltMV–eGFP [expressing eGFP from a duplicated sg CP promoter] are described elsewhere (Lim *et al.*, 2010a). To generate AltMV–eGFPACP, the sg promoter, CP and 3' untranslated region were amplified using *NheI* and *XbaI* primers and substituted into *NheI/XbaI*-digested AltMV–eGFP. The start codons of TGB2 and TGB3, and TGB3 aa 17 and 18, were mutated separately to create clones AltMV–eGFPΔTGB2, AltMV–eGFPΔTGB3 and AltMV–TGB3<sub>VL(17,18)AR</sub>–eGFP, respectively, using overlap PCR (Wurch *et al.*, 1998). When the TGB2 start codon was mutated, the TGB1 amino acid sequence was maintained; similarly, the TGB2 amino acid sequence was maintained when the TGB3 start codon was ablated and additional mutations were introduced. To generate a clone overexpressing TGB3, the TGB3 gene was amplified using primers adding *BamHI* and *NheI* sites at the 5' and 3' termini, respectively, and substituted for eGFP in AltMV–eGFP, forming AltMV(TGB3<sub>AltMV</sub>+) . A similar clone overexpressing PVX TGB3 was generated by substitution of PVX TGB3 amplified from pPC2S (Baulcombe *et al.*, 1995), forming AltMV(TGB3<sub>PVX</sub>+) . AltMVΔTGB3 was created as for AltMV–eGFPΔTGB3. AltMV TGB3 was amplified and inserted in place of eGFP in AltMV–eGFPΔTGB3 to form AltMVΔTGB3(TGB3+) ; AltMVΔTGB3(TGB3–GFP+) , expressing TGB3–GFP as an added gene, was created by replacing eGFP with TGB3–GFP, amplified from pHVLG–TGB3 (see below), into *BamHI/NheI*-digested AltMV–eGFP. AltMV TGB3 was amplified and inserted as a *BamHI/MluI* fragment into infectious clone PVX–MCS, forming PVX(TGB3<sub>AltMV</sub>+) ; PVX–MCS is a derivative of PVX infectious clone pPC2S, described elsewhere (Lim *et al.*, 2010b). PVX–MCS was modified separately to overexpress C-terminally 6 × His-tagged AltMV TGB3 and TGB3<sub>VL(17,18)AR</sub>, forming PVX(TGB3<sub>AltMV</sub>–His+) and PVX[TGB3<sub>VL(17,18)AR</sub>–His+] , respectively.

Full-length cDNA clones were linearized by using *XbaI* (AltMV clones) or *SpeI* (PVX clones) before *in vitro* transcription of infectious

RNA for *N. benthamiana* inoculation, using T7 RNA polymerase as described by Petty *et al.* (1989). Q-RT-PCR to quantify TGB3 RNA was performed as described by Bae *et al.* (2006) using TGB3-specific primers.

**Agrobacterium infiltration and transient expression constructs.** All binary vectors used were derived from pGD (to express free protein), pGDG (GFP–protein fusion) or pGDR (DsRed–protein fusion) as described by Goodin *et al.* (2002). The TGB2, TGB2/3 together, and TGB3 genes of AltMV were amplified and inserted into the *XhoI/BamHI* sites of appropriate vectors. TGB2 and TGB2/3 were inserted into pGD, forming pGD–TGB2 and pGD–TGB2/3, respectively. TGB3 was inserted into pGD (unfused TGB3) and into pGDG and pGDR to form N-terminal fusions (GFP–TGB3, DsRed–TGB3). PVX TGB3 was amplified from pPC2S using primers *XhoI-F/BamHI-R* and inserted into *XhoI/BamHI*-digested pGDG and pGDR, forming pGDG–TGB3<sub>PVX</sub> and pGDR–TGB3<sub>PVX</sub>. C-terminally fused eGFP was amplified from pEGFP-C1 (Clontech) using primers *KpnI-F/BamHI-R* and inserted into *KpnI/BamHI*-digested pGD vector, creating pHVLG. DsRed for C-terminal fusions was amplified from pGDR and inserted as a *KpnI/BamHI* fragment into pGD, creating pHVLR. TGB3 and deletion or substitution mutants were amplified with appropriate primers and cloned between the *XhoI/KpnI* or *HindIII/KpnI* sites of pHVLG and pHVLR, forming pHVLG–TGB3 (TGB3–GFP) and pHVLR–TGB3 (TGB3–DsRed) derivatives. All mutated sequences were verified by sequencing. Abaxial infiltrations of *N. benthamiana* leaves with *Agrobacterium tumefaciens* were performed essentially as described previously (Lim *et al.*, 2009), applying a final concentration of 0.6 OD<sub>600</sub>, with constructs mixed in equal proportions where appropriate.

**Detection and localization of fluorescent fusion proteins in *N. benthamiana*.** Leaf pieces and transverse sections (approx. 0.2 mm) of fresh leaves of *N. benthamiana* were examined with a Zeiss 710 laser-scanning confocal microscope system. An Argon laser was used to excite GFP at 488 nm and emission was monitored at 500–520 nm. DsRed was excited at 568 nm and emission was detected at 570–600 nm. Autofluorescence of chloroplasts was detected by using a 670 nm emission filter. Images were observed using an AxioObserver inverted microscope with a 40×1.2 NA water immersion Plan Apochromatic objective. DIC and fluorescence images were acquired simultaneously. The Zeiss Zen software package was used to capture images, and Zeiss AxioVision Release 4.8.3 with 4D software was used to construct three-dimensional images and calculate lateral sections from 35–60 optical slices of 1 µm in the Z dimension (Z-stack).

**Western blotting.** Total protein extracts from infected or agroinfiltrated *N. benthamiana* leaves were obtained by grinding fresh tissue in Smash buffer (Deng *et al.*, 2007) and boiling for 10 min. Protein extracts were run on 12 or 20% polyacrylamide gels and blotted onto PVDF membranes, followed by visualization using appropriate antibodies and chemiluminescent detection. AltMV-specific antibody was a gift of Andrew Geering (Geering & Thomas, 1999). Anti-GFP Living Colours monoclonal antibody (Clontech), anti-DsRed Living Colours monoclonal antibody (Clontech) and His tag monoclonal antibody (Sigma) were diluted as recommended by the manufacturers. Detection was by 1:2500-diluted horseradish peroxidase-conjugated goat anti-rabbit (PerkinElmer) or anti-mouse (Thermo) antibodies, with SuperSignal-WestFemto substrate (Thermo).

**Localization of viral RNA by FISH.** Leaf tissue collected from AltMV-infected *N. benthamiana* seedlings 20 days p.i. was processed to obtain paraffin sections for *in situ* hybridization, essentially as described by Zhu *et al.* (2001). Fluorescently labelled RNA probe complementary to the CP ORF of AltMV was prepared by *in vitro* transcription of linearized plasmid DNA in the presence of Alexa Fluor 488–UTP (Invitrogen). *In situ* hybridization was performed as

described by Zhu *et al.* (2001), using reagents from Boehringer Mannheim. In brief, dewaxed sections were pre-hybridized in blocking solution and incubated with labelled RNA probe. After washing, sections were mounted in ProLong Gold antifade solution (Invitrogen) and examined by LSCM as described above.

**Electron microscopy analysis of thin sections of *N. benthamiana* leaves.** Tissue samples (approx. 2×1 mm) were excised from infected leaves of *N. benthamiana* and processed for embedding according to Lawson & Heaton (1974). Ultrathin sections were examined with a JEOL 100CX II transmission electron microscope equipped with an HR digital camera system (Advanced Microscopy Techniques Corp.).

**Sequence analysis** The amino acid sequence of AltMV TGB3 was compared with those of homologues of related viruses by BLASTP analysis (NCBI), and conserved domains were examined by using the CDD option within NCBI (Marchler-Bauer *et al.*, 2007). TGB3 amino acid sequences of AltMV-SP (GenBank accession no. AAX86023.1), PVX (YP\_002332932.1), PapMV (AAG52895.1), WCIMV (NP\_620718.1), FMV (NP\_040991.1), BaMV (NP\_042586.1), CIYMV (NP\_077082.1), PLAMV (NP\_620839.1), TVX (NP\_702991.1) and ZVX (YP\_054405.1) were analysed further using Phobius software (Käll *et al.*, 2004, 2005; EMBL-EBI) to improve discrimination between the hydrophobic regions of a transmembrane helix and those of an SP. Additional comparisons were made using SignalP, TargetP and ChloroP (<http://www.cbs.dtu.dk/services/>), following the steps proposed by Emanuelsson *et al.* (2007).

## ACKNOWLEDGEMENTS

We wish to thank Michael Reinsel for excellent technical assistance. We also thank Peter Moffett for helpful comments and discussion during preparation of the manuscript.

## REFERENCES

- Adams, M. J., Antoniw, J. F., Bar-Joseph, M., Brunt, A. A., Candresse, T., Foster, G. D., Martelli, G. P., Milne, R. G., Zavriev, S. K. & Fauquet, C. M. (2004). The new plant virus family *Flexiviridae* and assessment of molecular criteria for species demarcation. *Arch Virol* **149**, 1045–1060.
- Bae, H., Kim, M. S., Sicher, R. C., Bae, H. J. & Bailey, B. A. (2006). Necrosis- and ethylene-inducing peptide from *Fusarium oxysporum* induces a complex cascade of transcripts associated with signal transduction and cell death in *Arabidopsis*. *Plant Physiol* **141**, 1056–1067.
- Bamunusinghe, D., Hemenway, C. L., Nelson, R. S., Sanderfoot, A. A., Ye, C. M., Silva, M. A. T., Payton, M. & Verchot-Lubicz, J. (2009). Analysis of potato virus X replicase and TGBp3 subcellular locations. *Virology* **393**, 272–285.
- Baulcombe, D. C., Chapman, S. & Santa Cruz, S. (1995). Jellyfish green fluorescent protein as a reporter for virus infections. *Plant J* **7**, 1045–1053.
- Beck, D. L., Guilford, P. J., Voot, D. M., Andersen, M. T. & Forster, R. L. (1991). Triple gene block proteins of white clover mosaic potyvirus are required for transport. *Virology* **183**, 695–702.
- Boevink, P. & Oparika, K. J. (2005). Virus–host interactions during movement processes. *Plant Physiol* **138**, 1815–1821.
- Deng, M., Bragg, J. N., Ruzin, S., Schichnes, D., King, D., Goodin, M. M. & Jackson, A. O. (2007). Role of the *Sonchus* yellow net virus N protein in formation of nuclear viroplasm. *J Virol* **81**, 5362–5374.
- Ding, B. (1998). Intercellular protein trafficking through plasmodesmata. *Plant Mol Biol* **38**, 279–310.

- Ding, X., Shintaku, M. H., Carter, S. A. & Nelson, R. S. (1996). Invasion of minor veins of tobacco leaves inoculated with tobacco mosaic virus mutants defective in phloem-dependent movement. *Proc Natl Acad Sci U S A* **93**, 11155–11160.
- Dolja, V. V., Haldeman, R., Robertson, N. L., Dougherty, W. G. & Carrington, J. C. (1994). Distinct functions of capsid protein in assembly and movement of tobacco etch potyvirus in plants. *EMBO J* **13**, 1482–1491.
- Donald, R. G., Zhou, H. & Jackson, A. O. (1993). Serological analysis of barley stripe mosaic virus-encoded proteins in infected barley. *Virology* **195**, 659–668.
- Emanuelsson, O., Brunak, S., von Heijne, G. & Nielsen, H. (2007). Locating proteins in the cell using TargetP, SignalP and related tools. *Nat Protoc* **2**, 953–971.
- Geering, A. D. & Thomas, J. E. (1999). Characterisation of a virus from Australia that is closely related to papaya mosaic potexvirus. *Arch Virol* **144**, 577–592.
- Goodin, M. M., Dietzgen, R. G., Schichnes, D., Ruzin, S. & Jackson, A. O. (2002). pGD vectors: versatile tools for the expression of green and red fluorescent protein fusions in agroinfiltrated plant leaves. *Plant J* **31**, 375–383.
- Hammond, J., Reinsel, M. D. & Maroon-Lango, C. J. (2006). Identification and full sequence of an isolate of *Alternanthera* mosaic potexvirus infecting *Phlox stolonifera*. *Arch Virol* **151**, 477–493.
- Haupt, S., Cowan, G. H., Ziegler, A., Roberts, A. G., Oparka, K. J. & Torrance, L. (2005). Two plant-viral movement proteins traffic in the endocytic recycling pathway. *Plant Cell* **17**, 164–181.
- Haywood, V., Kragler, F. & Lucas, W. J. (2002). Plasmodesmata: pathways for protein and ribonucleoprotein signaling. *Plant Cell* **14** (Suppl.), S303–S325.
- Ju, H. J., Samuels, T. D., Wang, Y. S., Blancaflor, E., Payton, M., Mitra, R., Krishnamurthy, K., Nelson, R. S. & Verchot-Lubicz, J. (2005). The potato virus X TGBp2 movement protein associates with endoplasmic reticulum-derived vesicles during virus infection. *Plant Physiol* **138**, 1877–1895.
- Ju, H. J., Ye, C. M. & Verchot-Lubicz, J. (2008). Mutational analysis of PVX TGBp3 links subcellular accumulation and protein turnover. *Virology* **375**, 103–117.
- Käll, L., Krogh, A. & Sonnhammer, E. L. L. (2004). A combined transmembrane topology and signal peptide prediction method. *J Mol Biol* **338**, 1027–1036.
- Käll, L., Krogh, A. & Sonnhammer, E. L. L. (2005). An HMM posterior decoder for sequence feature prediction that includes homology information. *Bioinformatics* **21** (Suppl. 1), i251–i257.
- Krishnamurthy, K., Heppler, M., Mitra, R., Blancaflor, E., Payton, M., Nelson, R. S. & Verchot-Lubicz, J. (2003). The potato virus X TGBp3 protein associates with the ER network for virus cell-to-cell movement. *Virology* **309**, 135–151.
- Lauber, E., Jonard, G., Richards, K. & Guilley, H. (2005). Nonregulated expression of TGBp3 of hordei-like viruses but not of potex-like viruses inhibits beet necrotic yellow vein virus cell-to-cell movement. *Arch Virol* **150**, 1459–1467.
- Lawson, R. H. & Hearon, S. S. (1974). Ultrastructure of carnation etched ring virus-infected *Saponaria vaccaria* and *Dianthus caryophyllus*. *J Ultrastruct Res* **48**, 201–215.
- Leisner, S. M. & Howell, S. H. (1993). Long-distance movement of viruses in plants. *Trends Microbiol* **1**, 314–317.
- Lim, H. S., Bragg, J. N., Ganesan, U., Lawrence, D. M., Yu, J., Isogai, M., Hammond, J. & Jackson, A. O. (2008). Triple gene block protein interactions involved in movement of barley stripe mosaic virus. *J Virol* **82**, 4991–5006.
- Lim, H. S., Bragg, J. N., Ganesan, U., Ruzin, S., Schichnes, D., Lee, M. Y., Vaira, A. M., Ryu, K. H., Hammond, J. & Jackson, A. O. (2009). Subcellular localization of the barley stripe mosaic virus triple gene block proteins. *J Virol* **83**, 9432–9448.
- Lim, H.-S., Vaira, A. M., Reinsel, M. D., Bae, H., Bailey, B. A., Domier, L. L. & Hammond, J. (2010a). Localization of *Alternanthera* mosaic virus pathogenicity determinants to RdRp and TGB1, and separation of TGB1 silencing suppression from movement functions. *J Gen Virol* **91**, 277–287.
- Lim, H.-S., Vaira, A. M., Domier, L. L., Kim, H. G. & Hammond, J. (2010b). Efficiency of VIGS and gene expression in a novel bipartite potexvirus vector delivery system as a function of strength of TGB1 silencing suppression. *Virology* **402**, 149–163.
- Lin, M. K., Hu, C. C., Lin, N. S., Chang, B. Y. & Hsu, Y. H. (2006). Movement of potexviruses requires species-specific interactions among the cognate triple gene block proteins, as revealed by a *trans*-complementation assay based on the bamboo mosaic virus satellite RNA-mediated expression system. *J Gen Virol* **87**, 1357–1367.
- Lough, T. J. & Lucas, W. J. (2006). Integrative plant biology: role of phloem long-distance macromolecular trafficking. *Annu Rev Plant Biol* **57**, 203–232.
- Lough, T. J., Shash, K., Xoconostle-Cázares, B., Hofstra, K. R., Beck, D. L., Balmori, E., Forster, R. L. S. & Lucas, W. J. (1998). Molecular dissection of the mechanism by which potexvirus triple gene block proteins mediate cell-to-cell transport of infectious RNA. *Mol Plant Microbe Interact* **11**, 801–814.
- Lough, T. J., Netzler, N. E., Emerson, S. J., Sutherland, P., Carr, F., Beck, D. L., Lucas, W. J. & Forster, R. L. (2000). Cell-to-cell movement of potexviruses: evidence for a ribonucleoprotein complex involving the coat protein and first triple gene block protein. *Mol Plant Microbe Interact* **13**, 962–974.
- Lough, T. J., Lee, R. H., Emerson, S. J., Forster, R. L. & Lucas, W. J. (2006). Functional analysis of the 5' untranslated region of potexvirus RNA reveals a role in viral replication and cell-to-cell movement. *Virology* **351**, 455–465.
- Lucas, W. J. (2006). Plant viral movement proteins: agents for cell-to-cell trafficking of viral genomes. *Virology* **344**, 169–184.
- Lucas, W. J., Yoo, B. C. & Kragler, F. (2001). RNA as a long-distance information macromolecule in plants. *Nat Rev Mol Cell Biol* **2**, 849–857.
- Marchler-Bauer, A., Anderson, J. B., Derbyshire, M. K., DeWeese-Scott, C., Gonzales, N. R., Gwadz, M., Hao, L., He, S., Hurwitz, D. I. & other authors (2007). CDD: a conserved domain database for interactive domain family analysis. *Nucleic Acids Res* **35**, D237–D240.
- Morozov, S. Yu. & Solovyev, A. G. (2003). Triple gene block: modular design of a multifunctional machine for plant virus movement. *J Gen Virol* **84**, 1351–1366.
- Morozov, S. Yu., Miroshnichenko, N. A., Solovyev, A. G., Zelenina, D. A., Fedorkin, O. N., Lukashcheva, L. I., Grachev, S. A. & Chernov, B. K. (1991). *In vitro* membrane binding of the translation products of the carlavirus 7-kDa protein genes. *Virology* **183**, 782–785.
- Morozov, S. Yu., Fedorkin, O. N., Jüttner, G., Schiemann, J., Baulcombe, D. C. & Atabekov, J. G. (1997). Complementation of a potato virus X mutant mediated by bombardment of plant tissues with cloned viral movement protein genes. *J Gen Virol* **78**, 2077–2083.
- Petty, I. T., Hunter, B. G., Wei, N. & Jackson, A. O. (1989). Infectious barley stripe mosaic virus RNA transcribed *in vitro* from full-length genomic cDNA clones. *Virology* **171**, 342–349.
- Prod'homme, D., Jakubiec, A., Tournier, V., Drugeon, G. & Jupin, I. (2003). Targeting of the turnip yellow mosaic virus 66K replication protein to the chloroplast envelope is mediated by the 140K protein. *J Virol* **77**, 9124–9135.
- Rubino, L. & Russo, M. (1998). Membrane targeting sequences in tombusvirus infections. *Virology* **252**, 431–437.

- Sakaguchi, M., Tomiyoshi, R., Kuroiwa, T., Mihara, K. & Omura, T. (1992).** Functions of signal and signal-anchor sequences are determined by the balance between the hydrophobic segment and the N-terminal charge. *Proc Natl Acad Sci U S A* **89**, 16–19.
- Samuels, T. D., Ju, H. J., Ye, C. M., Motes, C. M., Blancaflor, E. B. & Verchot-Lubicz, J. (2007).** Subcellular targeting and interactions among the potato virus X TGB proteins. *Virology* **367**, 375–389.
- Schepetilnikov, M. V., Manske, U., Solovyev, A. G., Zamyatnin, A. A., Jr, Schiemann, J. & Morozov, S. Y. (2005).** The hydrophobic segment of potato virus X TGBp3 is a major determinant of the protein intracellular trafficking. *J Gen Virol* **86**, 2379–2391.
- Solovyev, A. G., Stroganova, T. A., Zamyatnin, A. A., Jr, Fedorkin, O. N., Schiemann, J. & Morozov, S. Y. (2000).** Subcellular sorting of small membrane-associated triple gene block proteins: TGBp3-assisted targeting of TGBp2. *Virology* **269**, 113–127.
- Tamai, A. & Meshi, T. (2001).** Tobamoviral movement protein transiently expressed in a single epidermal cell functions beyond multiple plasmodesmata and spreads multicellularly in an infection-coupled manner. *Mol Plant Microbe Interact* **14**, 126–134.
- Torrance, L., Cowan, G. H., Gillespie, T., Ziegler, A. & Lacomme, C. (2006).** Barley stripe mosaic virus-encoded proteins triple-gene block 2 and  $\gamma$ b localize to chloroplasts in virus-infected monocot and dicot plants, revealing hitherto-unknown roles in virus replication. *J Gen Virol* **87**, 2403–2411.
- Verchot-Lubicz, J. (2005).** A new cell-to-cell transport model for potexviruses. *Mol Plant Microbe Interact* **18**, 283–290.
- Verchot-Lubicz, J., Ye, C. M. & Bamunusinghe, D. (2007).** Molecular biology of potexviruses: recent advances. *J Gen Virol* **88**, 1643–1655.
- von Heijne, G. (1988).** Transcending the impenetrable: how proteins come to terms with membranes. *Biochim Biophys Acta* **947**, 307–333.
- Wagmann, E., Ueki, S. & Trutnyeva, K. (2004).** The ins and outs of nondestructive cell-to-cell and systemic movement of plant viruses. *CRC Crit Rev Plant Sci* **23**, 195–250.
- Wurch, T., Lestienne, F. & Pauwels, P. (1998).** A modified overlap extension PCR method to create chimeric genes in the absence of restriction enzymes. *Biotechnol Tech* **12**, 653–657.
- Xiong, Z., Kim, K. H., Giesman-Cookmeyer, D. & Lommel, S. A. (1993).** The roles of the red clover necrotic mosaic virus capsid and cell-to-cell movement proteins in systemic infection. *Virology* **192**, 27–32.
- Zhu, Y., Green, L., Woo, Y.-M., Owens, R. A. & Ding, B. (2001).** Cellular basis of potato spindle tuber viroid systemic movement. *Virology* **279**, 69–77.